AGU PUBLICATIONS

Geophysical Research Letters

RESEARCH LETTER
10.1002/2015GL064320

Key Points:
- Warming climate slightly increases the carbon inventory of the Southern Ocean
- Regenerated carbon is increased in the deep water
- The intensified wind increases anthropogenic carbon uptake

Supporting Information:
- Support Information S1

Correspondence to:
T. Ito,
taka.ito@eas.gatech.edu

Citation:
Ito, T., A. Bracco, C. Deutsch, H. Frenzel, M. Long, and Y. Takano (2015), Sustained growth of the Southern Ocean carbon storage in a warming climate, *Geophys. Res. Lett.*, *42*, doi:10.1002/2015GL064320.

Received 21 APR 2015
Accepted 18 MAY 2015
Accepted article online 21 MAY 2015

Sustained growth of the Southern Ocean carbon storage in a warming climate

Takamitsu Ito[1], Annalisa Bracco[1], Curtis Deutsch[2], Hartmut Frenzel[2], Matthew Long[3], and Yohei Takano[1]

[1]School of Earth and Atmospheric Sciences, Georgia Institute of Technology, Atlanta, Georgia, USA, [2]School of Oceanography, University of Washington, Seattle, Washington, USA, [3]Climate and Global Dynamics Division, National Center for Atmospheric Research, Boulder, Colorado, USA

Abstract We investigate the mechanisms controlling the evolution of Southern Ocean carbon storage under a future climate warming scenario. A subset of Coupled Model Intercomparison Project Phase 5 models predicts that the inventory of biologically sequestered carbon south of 40°S increases about 18–34 Pg C by 2100 relative to the preindustrial condition. Sensitivity experiments with an ocean circulation and biogeochemistry model illustrates the impacts of the wind and buoyancy forcings under a warming climate. Intensified and poleward shifted westerly wind strengthens the upper overturning circulation, not only leading to an increased uptake of anthropogenic CO_2 but also releasing biologically regenerated carbon to the atmosphere. Freshening of Antarctic Surface Water causes a slowdown of the lower overturning circulation, leading to an increased Southern Ocean biological carbon storage. The rectified effect of these processes operating together is the sustained growth of the carbon storage in the Southern Ocean, even under the warming climate with a weaker global ocean carbon uptake.

1. Motivation

The oceans are by far the largest carbon reservoir in the climate system. Approximately one third of the anthropogenic carbon dioxide emitted by human activities has been absorbed into the global oceans [*Khatiwala et al.*, 2009] mitigating the anthropogenic greenhouse emissions. Approximately 40% of the oceanic carbon uptake has occurred in the Southern Ocean due to the vigorous exchange of surface and deep waters and the formation of intermediate and mode waters by the overturning circulations [*Marshall and Speer*, 2012]. Anthropogenic carbon absorbed in the Southern Ocean is mainly exported to and stored in the Southern Hemisphere subtropical thermocline [*Ito et al.*, 2010; *Mignone et al.*, 2006; *Sabine et al.*, 2004; *Sallee et al.*, 2012].

In this work we analyze changes in the surface climate and carbon content of the Southern Ocean in Earth System Model (ESM) simulations performed as a part of Coupled Model Intercomparison Project Phase 5 (CMIP-5) under the Representative Concentration Pathway 8.5 (RCP8.5) scenario. The selected models have diverse representations of a wide range of climate and marine biogeochemical processes. Predictions that are common across models in spite of the structural and/or parametric differences between them are more likely to be robust. According to these models, the surface waters between 45°S and 60°S are predicted to become warmer and fresher, and the near-surface winds to intensify toward the end of the 21st century (Figure 1), leading to perturbations in the physical oceanographic circulation [*Meijers*, 2014]. Those tendencies are common to all models, despite significant differences in the representation of the mean climatologies, The increased stratification may weaken formation of deep water masses, thereby weakening in turn the uptake of anthropogenic carbon [*Sarmiento et al.*, 1998]. In contrast, the intensification and poleward shifting of the westerly wind [*Thompson et al.*, 2011] may intensify the upper overturning circulation [*Waugh et al.*, 2013], increasing the supply of carbon-rich deep water to the surface and releasing excess carbon to the atmosphere [*Le Quéré et al.*, 2007; *Lovenduski et al.*, 2013]. At the same time, the increased wind-driven circulation may augment the equatorward transfer and subduction of anthropogenic carbon into the thermocline [*Ito et al.*, 2010; *Sallee et al.*, 2012]. Therefore, the future of the Southern Ocean carbon uptake will depend on the simultaneous changes in the surface buoyancy and wind forcings and on how the ocean circulation will respond to them.

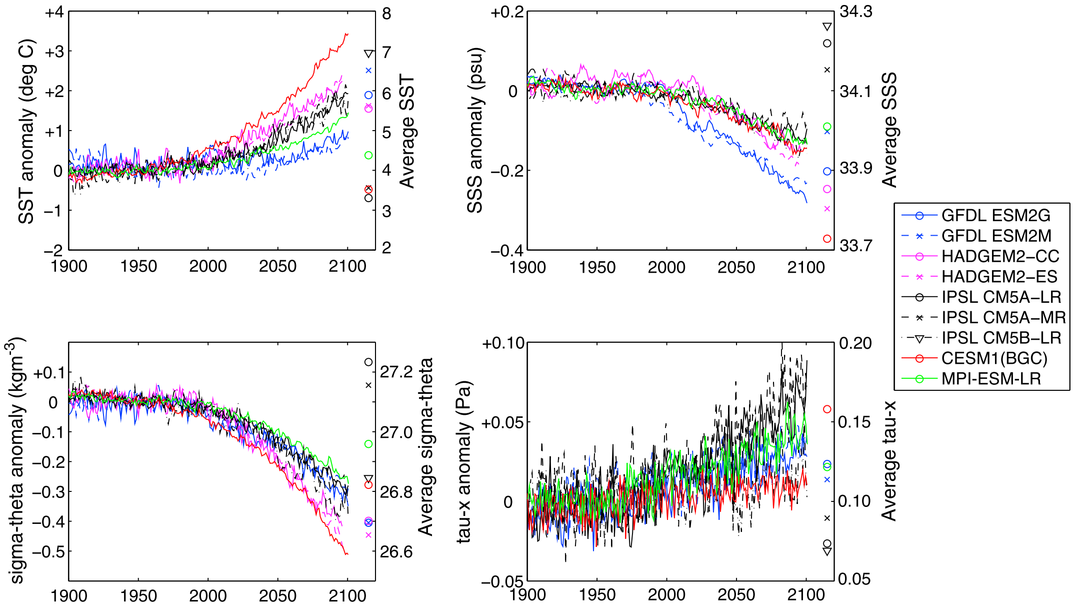

Figure 1. Area-weighted annual mean surface properties over the extratropical Southern Hemisphere oceans (45°S–60°S, 1900 to 2100) relative to the averages from 1950 to 1960 (shown on the right axes). (top left) Sea surface temperature in °C, (top right) sea surface salinity in practical salinity unit, (bottom left) surface density anomaly in kg m^{-3}, and (bottom right) zonal wind stress in pascal. CMIP-5 models are color coded (blue solid line = GFDL-ESM2G and blue dashed line = GFDL-ESM2M [*Dunne et al.*, 2012], magenta solid line = HADGEM2-CC, magenta dashed line = HADGEM2-ES [*Collins et al.*, 2011], black solid line = IPSL CM5A-LR, black dashed line = IPSL CM5A-MR, black dash-dotted line = IPSL CM5B-LR [*Dufresne et al.*, 2013], red solid line = CESM1(BGC) [*Long et al.*, 2013; *Moore et al.*, 2013], and green solid line = MPI-ESM-LR [*Giorgetta et al.*, 2013]).

Inferences from the observations are equivocal. Atmospheric inversions indicate a weakened Southern Ocean carbon uptake since the 1980s potentially associated with the intensified and poleward shifted westerly wind [*Le Quéré et al.*, 2007] but are subject to large uncertainty due to sparse observations and atmospheric transport biases. In contrast, shipboard measurements of air-sea disequilibrium of CO_2 have not changed significantly over decadal timescales, indicating a persistent sink [*Fay and McKinley*, 2013]. On the intraseasonal timescale, the Ekman transport indeed links the regional carbon fluxes to variability in atmospheric wind stress forcing [*Butler et al.*, 2007]. However, on longer timescales, the oceanic response is more complex as the eddy activity may compensate the effect of wind variability [*Boning et al.*, 2008; *Meredith et al.*, 2012; *Meredith and Hogg*, 2006], potentially reducing the upwelling of excess carbon.

2. Simulated Southern Ocean Carbon Storage in the CMIP-5 Models

Future projections of the carbon inventory south of 40°S are analyzed using the suite of CMIP-5 model outputs. The regional carbon inventory reflects the combined effects of air-sea CO_2 flux and the lateral convergence of ocean transport. We estimate the partitioning of the carbon inventory into the “preformed” and “regenerated” components based on the different pathways through which the carbon is transported vertically in the ocean. Preformed carbon is sequestered through the physical circulation carrying the dissolved inorganic carbon from the surface downward. In contrast, regenerated carbon is sequestered through photosynthetic formation of organic materials that subsequently sink downward and dissolve back to the inorganic form at depth. The degree of oxygen deficit relative to atmospheric saturation can be used to evaluate the regenerated carbon assuming a constant elemental stoichiometric ratio. A relatively smaller but nonetheless significant amount of regenerated carbon is also sequestered through the formation of calcium carbonate particles; this component of regenerated carbon can be estimated by computing the excess alkalinity in the subsurface waters [*Brewer*, 1978].

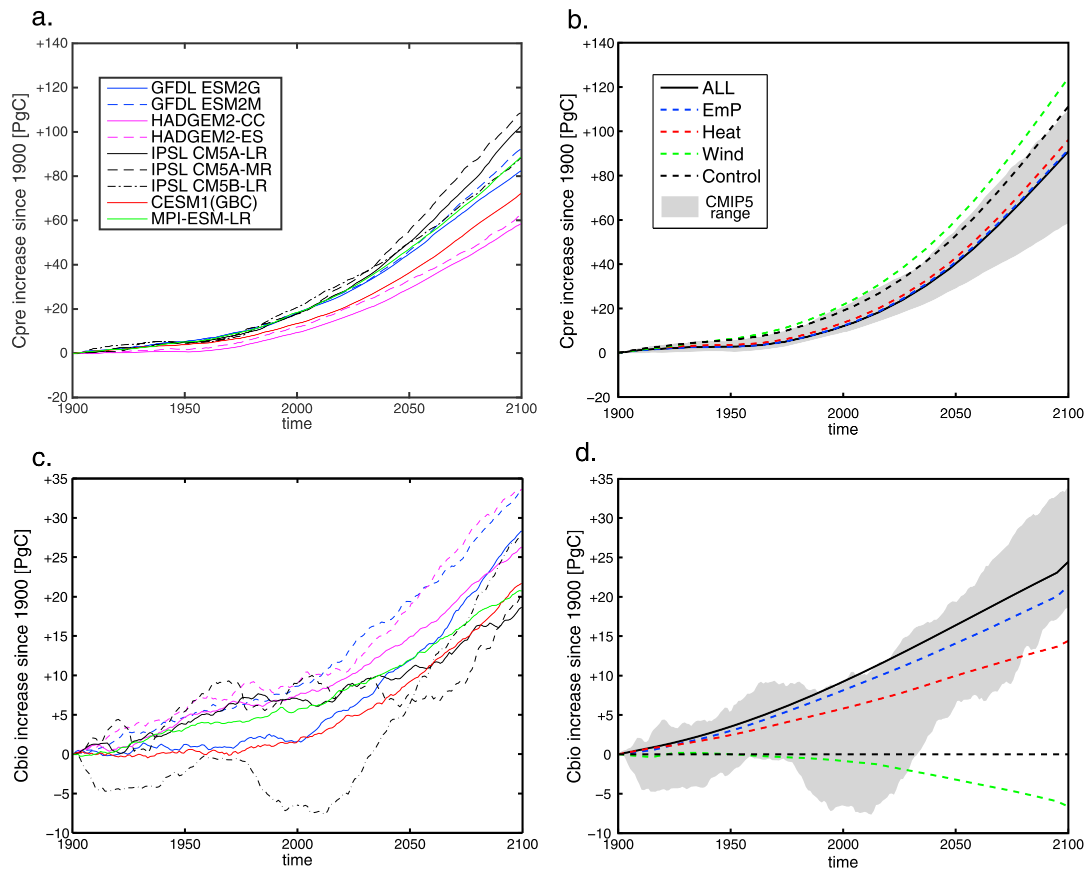

Figure 2. Southern Ocean carbon inventory change (in Pg C) since 1900 in the subset of the CMIP-5 archive. (a) Preformed carbon and (c) regenerated carbon are plotted in the same color coding as Figure 1. The results of the sensitivity experiments: (b) Preformed carbon and (d) regenerated carbon are plotted over the simulated range of CMIP-5 output (shading). The line types and colors are black solid = all forcings, blue dashed = freshwater forcing, red dashed = thermal forcing, and green dashed = wind forcing.

Both preformed and regenerated carbon inventories increase in the Southern Ocean from the recent past toward the end of this century (Figures 2a and 2c). The preformed carbon inventory rises at the multimodel median rate of 88.2 Pg C (mean, STD, IQR = 83.9, 17.0, 25.1 Pg C) from the year 1900 to 2100, whereas the regenerated component rises at the median rate of 26.3 Pg C (mean, STD, IQR = 25.7, 5.7, 9.0 Pg C). The preformed component increases primarily in the upper ocean thermocline as it is mainly driven by uptake associated with soaring atmospheric CO_2. The regenerated carbon inventory shows relatively larger model-to-model differences, but all models eventually predict increased carbon stock toward the end of the 21st century.

3. Sensitivity Experiments Using an Ocean Circulation and Carbon Cycle Model

What are the mechanisms responsible for the increased storage of preformed and regenerated carbon in the Southern Ocean? To illustrate the processes behind the changing carbon storage, we performed a suite of numerical sensitivity experiments that mimic some common features of the centennial scale, global warming simulations using a relatively simple, ocean-only general circulation (OGCM) and carbon cycle model described in the supporting information. We separately consider the influences of ocean warming, acceleration of the hydrological cycle, and intensified southern westerly winds. Atmospheric pCO_2 was set to increase following observations from 1900 to 2005 and then the RCP8.5 scenario from 2005 to 2100 for all idealized model runs. A control simulation is first performed without any physical perturbation, but subject to rising atmospheric pCO_2. The sensitivity runs were performed as follows: the warming perturbation (Heat) uniformly increases the sea surface temperature at the rate of 1°C per century; the freshwater perturbation (EmP) amplifies the evaporation minus precipitation field at a rate of 10% per century while keeping its spatial pattern the same; The wind perturbation experiment (Wind) shifts the Southern Ocean wind stress poleward by about 1°latitude per century and intensifies its amplitude about 10% per century, using the Southern Annular Mode-regressed Southern Hemisphere wind stress. These perturbations are purposefully kept simple to facilitate understanding of the underlying mechanisms, while mimicking the overall trajectory of more realistic climate model simulations [*Capotondi et al*., 2012; *Meijers*, 2014].

Despite its simplicity, the model broadly reproduces the evolution of preformed and regenerated carbon storage as simulated by the CMIP-5 climate-carbon models when all perturbations are imposed concurrently (ALL runs in Figures 2b and 2d). The total carbon storage south of 40°S increases by 114 Pg C (explained by the preformed and regenerated components for 89.6 and 29.4 Pg C, respectively) over the 200 year period, which is slightly greater than the control run increase of 109 Pg C (entirely explained by the preformed component). Under the combined effect of the physical perturbations, the regional carbon storage increases slightly (+5.1 Pg C); in contrast, the global oceanic carbon uptake weakens by −37.6 Pg C, which is consistent with the climate-driven reduction of the global oceanic carbon storage in the CMIP-5 models [*Boer and Arora*, 2012]. Thus, the carbon stock of the Southern Ocean regionally resists the global-scale weakening of the oceanic carbon uptake.

What sustains the growth of Southern Ocean carbon storage? The climate-induced carbon storage increase from 1900 to 2100 (+5.1 Pg C) represents a residual between the decline in the preformed carbon (−19.7 Pg C, ALL minus Control in Figure 2b) and the increase in regenerated carbon (+24.4 Pg C, ALL minus Control in Figure 2d). The sensitivity experiments can further illustrate the different roles played by physical and biogeochemical processes. The effects of heating and freshening reduce the preformed carbon stock by −14.8 Pg C (Heat in Figure 2b) and −18.9 Pg C (EmP in Figure 2b), respectively, while the intensification of the westerly wind increases it by +13.3 Pg C (Wind in Figure 2b), relative to the control run. In contrast to the preformed carbon, regenerated carbon is independent of atmospheric CO_2 (there are no acidification feedbacks on the biological pump represented in this particular model), and any change in this component is due to the biogeochemical response to the changing climate. Heating and freshening contribute to an increase of the regenerated carbon stock by +13.6 Pg C (Heat in Figure 2d) and +20.8 Pg C (EmP in Figure 2d), respectively, while the intensification of the westerly wind slightly decreases it by −6.3 Pg C (Wind in Figure 2d), all relative to the control run. The interaction between the forcings is weakly nonlinear, and the sum of individual responses is slightly larger O(10%) than the combined response.

4. Underlying Mechanisms for Carbon Storage

Open-ocean deep convection in the Weddell Sea is a recurrent feature among the CMIP-5 models under preindustrial conditions but weakens and then ceases under a climate warming scenario owing to surface freshening [*de Lavergne et al*., 2014]. This produces an overall decline of the preformed carbon growth due to decreased solubility and weakened ventilation, driven by the buoyancy forcing (see supporting information figures). While the freshwater forcing tends to weaken the lower overturning cell of the Southern Ocean, the thermal forcing tends to weaken the sinking in the North Atlantic, which increases the age of the Circumpolar Deep Water even though there is little change in the regional Southern Ocean overturning (see Figure S2 in the supporting information). This reinforces the effect of freshwater forcing in the accumulation of regenerated carbon in the deep Southern Ocean. This effect is partially compensated by the intensification of the wind-driven circulation sequestering more anthropogenic carbon in the intermediate and mode waters.

The weakened deep ventilation also increases the regenerated carbon stock. The diverse temporal trajectories in Figure 2c may reflect the varying timing of the cessation of deep convection among the CMIP-5 models as revealed by *de Lavergne et al*. [2014]. The sensitivity experiments showed that the increase in the regenerated carbon stock slightly overwhelms the decline in the preformed component such that the net response is a small increase, thus the leading cause of the sustained increase in the regional storage is the buoyancy-driven weakening of the deep ventilation.

To further illustrate the operation of these compensating processes, we construct a simple box model that relates the intensity of the upper and lower overturning circulations to the age of the deep water in the

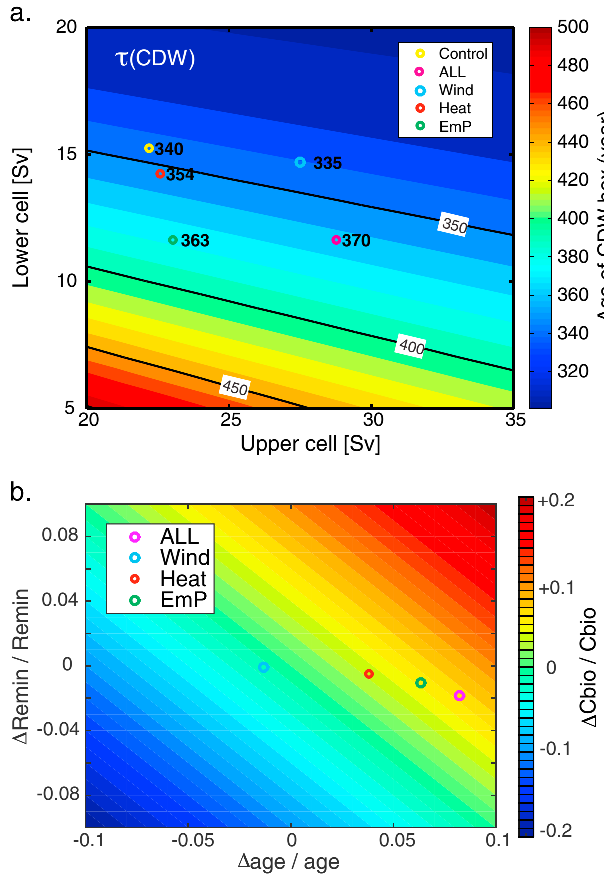

Figure 3. (a) Age of the CDW (in year) as a function of the upper and lower cell intensity. Color shading is the equilibrium solution from the box model (see Figure S1 in the supporting information), and the dots indicate the results from the sensitivity experiments. (b) Scaling for the regenerated carbon and water mass age of the CDW. The remineralization rate was diagnosed by taking the ratio between Cbio and water age averaged south of 40°S below 400 m.

Southern Ocean (see supporting information figures). The box model calculates the ventilation age of the bulk circumpolar deep water based on the intensity of the two overturning cells; these are prescribed and varied over a broad range. The box model successfully reproduces the character of the response simulated by the OGCM in the sensitivity experiments (Figure 3a). Just as in the OGCM, weakening of the lower overturning cell increases the age of the deep Southern Ocean, which can be partially compensated by intensification of the upper overturning cell. In the box model, we can estimate regenerated carbon storage (C_{reg}) considering the product of average respiration rate (R) and the age of the water (τ). The fractional change in regenerated carbon storage, then, is a linear combination of the changes in water mass age and respiration rate, $\frac{\Delta C_{reg}}{C_{reg}} = \frac{\Delta R}{R} + \frac{\Delta \tau}{\tau}$. Examining the sensitivity experiments in the context of the box model results shows that the increase in the regenerated carbon storage is primarily driven by the increasing age of circumpolar deep water (Figure 3b), which is driven by the buoyancy forcing. In the sensitivity experiments, the weakened deep ventilation is also accompanied by a slight decrease in the respiration rates, which may be induced by the reduction in the vertical supply of nutrients. However, the respiration rate decline offsets the age related changes only to a small degree, and the net outcome is still an accumulation of the regenerated carbon in the deep, less ventilated waters.

5. Discussion

The ability of the ocean to absorb atmospheric carbon dioxide in the coming century will globally decrease under a warming climate due to changes in the ocean circulation. The Southern Ocean resists this global trend through a sustained growth of the deep ocean carbon storage, which is driven by the retention of regenerated carbon at depth due to the weakened deep ventilation. Our analysis of a representative sample of CMIP-5 models reveal that in the near future in the Southern Ocean the deep overturning circulation will weaken, the upper overturning circulation will intensify, and the regenerated carbon stock will increase, in agreement with the recent work by *Bernardello et al*. [2014], *Meijers* [2014], and *de Lavergne et al*. [2014].

The simulated change in air-sea CO_2 flux (Figure 4) and the regional carbon inventory (Figure 2) further reveal the subtle balance in the carbon changes in the Southern Ocean. The natural component of air-sea CO_2 flux shows increased degassing under increasing SST and stronger wind-driven upper ocean ventilation, partially compensated by the weakened deep ventilation due to the freshening effect. The anthropogenic carbon uptake increases primarily due to the stronger wind-driven upper ocean ventilation. The net (anthropogenic and natural) effect is a moderate reduction (Figure 4d, dashed line) of carbon uptake

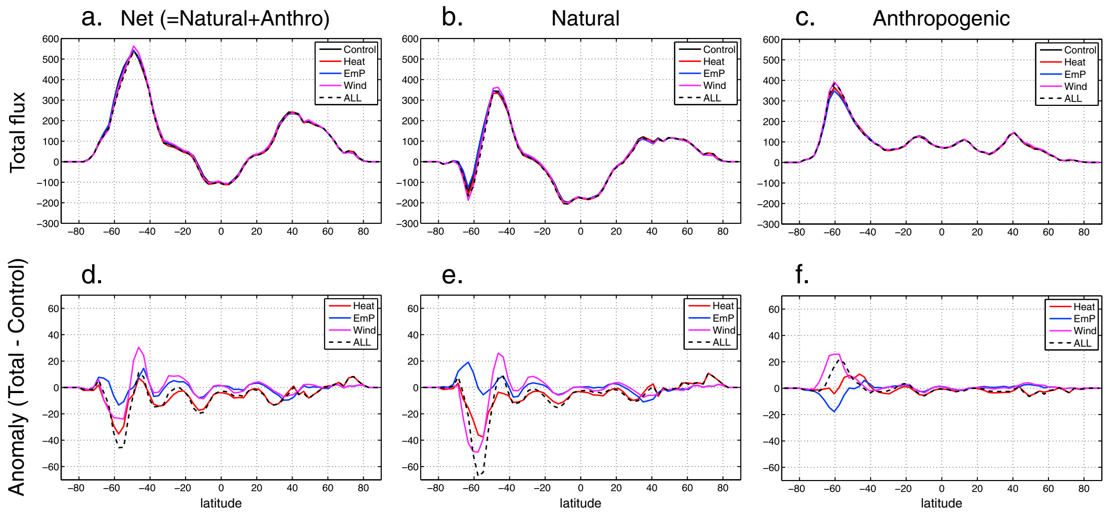

Figure 4. Temporally integrated zonal mean air-to-sea CO_2 flux from 1900 to 2100. Positive values indicate oceanic uptake. Natural simulations are forced with the preindustrial atmospheric pCO_2 of 278 ppmv, and anthropogenic fluxes are inferred by taking the difference between the total and natural fluxes. (a–c) The total flux and (d–f) are the perturbation from the control showing the changes induced by the climate perturbations. Figures 4a and 4d show the net air-sea flux which is the sum of natural (Figures 4b and 4e) and anthropogenic (Figures 4c and 4f) components.

(−12.4PgC) integrated south of 40°S. There is a discrepancy between the reduction of the integrated air-to-sea CO_2 flux and the increase in the carbon inventory of the same region (+5.1 Pg C). The difference must be explained by the lateral redistribution of carbon inventory across 40°S. While the carbon accumulates south of 40°S, the effect of reduced uptake must decrease the carbon inventory in the north of 40°S. The increased carbon inventory south of 40°S is primarily driven by the retention of regenerated carbon there, which indeed weakens the degassing of natural carbon as indicated by the blue line in Figure 4e.

Our results point to the importance of the dynamics of upper and lower overturning circulations as they are closely relevant to the water mass formation processes that mediate carbon biogeochemistry in the Southern Ocean and consequently to its carbon cycling. However, some of the crucial outstanding issues that have been neglected in this work due to the models' resolution and setup include the realism in representation of ocean eddies, turbulent mixed layer, sea ice, deep convection, and ocean mixing processes. Similarly, the response of biogeochemical and ecological processes to the changing climate are poorly understood and crudely parameterized.

These potential issues notwithstanding, the state-of-the-art models consistently show that the net increase in the regenerated carbon stock ultimately depends on the residual between the two opposing influences of weakened deep ventilation due to buoyancy forcing and strengthened upper overturning circulation due to the intensified winds. Equally important is the compensation between anthropogenic and natural carbon fluxes. Such compensation amplifies uncertainty in the net effect, since the uncertainties in each contributing dynamical and biogeochemical process are superimposed; this is illustrated by the complex and diverse behavior of the carbon storage as well as the air-sea CO_2 fluxes. Finally, while the sustained carbon storage in the Southern Ocean helps to moderate diminishing global uptake, it also accelerates the acidification in this region. Furthermore, the weakened ventilation and increased regenerated carbon stock implies declining oxygen levels through the respiratory oxygen loss, which poses additional environmental concerns.

Acknowledgments
This work is a result of the collaboration through the joint US-CLIVAR/OCB working group on the Ocean Carbon Uptake. Two anonymous reviewers provided helpful comments to improve the earlier version of this manuscript. We acknowledge the World Climate Research Programme's Working Group on Coupled Modelling, which is responsible for CMIP, and we thank the climate modeling groups (listed in Table S1 in supporting information) for producing and making available their model output. For CMIP the U.S. Department of Energy's Program for Climate Model Diagnosis and Intercomparison provides coordinating support and led development of software infrastructure in partnership with the Global Organization for Earth System Science Portals. All model diagnostics are archived by the corresponding author and can be provided by request. T.I. and Y.T. are supported by NSF OPP-1142009.

The Editor thanks two anonymous reviewers for their assistance in evaluating this paper.

References

Bernardello, R., I. Marinov, J. B. Palter, J. L. Sarmiento, E. D. Galbraith, and R. D. Slater (2014), Response of the ocean natural carbon storage to projected twenty-first-century climate change, *J. Clim.*, *27*(5), 2033–2053, doi:10.1175/JCLI-D-13-00343.1.

Boer, G. J., and V. K. Arora (2012), Feedbacks in emission-driven and concentration-driven global carbon budgets, *J. Clim.*, *26*(10), 3326–3341, doi:10.1175/JCLI-D-12-00365.1.

Boning, C. W., A. Dispert, M. Visbeck, S. R. Rintoul, and F. U. Schwarzkopf (2008), The response of the Antarctic Circumpolar Current to recent climate change, *Nat. Geosci.*, *1*(12), 864–869, doi:10.1038/ngeo362.

Brewer, P. G. (1978), Direct observation of the oceanic CO2 increase, *Geophys. Res. Lett.*, *5*(12), 997–1000, doi:10.1029/GL005i012p00997.

Butler, A. H., D. W. J. Thompson, and K. R. Gurney (2007), Observed relationships between the Southern Annular Mode and atmospheric carbon dioxide, *Global Biogeochem. Cycles*, *21*, GB4014, doi:10.1029/2006GB002796.

Capotondi, A., M. A. Alexander, N. A. Bond, E. N. Curchitser, and J. D. Scott (2012), Enhanced upper ocean stratification with climate change in the CMIP3 models, *J. Geophys. Res.*, *117*, C04031, doi:10.1029/2011JC007409.

Collins, W. J., et al. (2011), Development and evaluation of an Earth-System model—HadGEM2, *Geosci. Model Dev.*, *4*(4), 1051–1075, doi:10.5194/gmd-4-1051-2011.

de Lavergne, C., J. B. Palter, E. D. Galbraith, R. Bernardello, and I. Marinov (2014), Cessation of deep convection in the open Southern Ocean under anthropogenic climate change, *Nat. Clim. Change*, *4*(4), 278–282, doi:10.1038/nclimate2132.

Dufresne, J. L., et al. (2013), Climate change projections using the IPSL-CM5 Earth System Model: From CMIP3 to CMIP5, *Clim. Dyn.*, *40*(9–10), 2123–2165, doi:10.1007/s00382-012-1636-1.

Dunne, J. P., et al. (2012), GFDL's ESM2 global coupled climate–Carbon Earth System Models. Part II: Carbon system formulation and baseline simulation characteristics*, *J. Clim.*, *26*(7), 2247–2267, doi:10.1175/JCLI-D-12-00150.1.

Fay, A. R., and G. A. McKinley (2013), Global trends in surface ocean pCO_2 from in situ data, *Global Biogeochem. Cycles*, *27*, 541–557, doi:10.1002/gbc.20051.

Giorgetta, M. A., et al. (2013), Climate and carbon cycle changes from 1850 to 2100 in MPI-ESM simulations for the Coupled Model Intercomparison Project phase 5, *J. Adv. Model. Earth Syst.*, *5*, 572–597, doi:10.1002/jame.20038.

Ito, T., M. Woloszyn, and M. Mazloff (2010), Anthropogenic carbon dioxide transport in the Southern Ocean driven by Ekman flow, *Nature*, *463*(7277), 80–83, doi:10.1038/Nature08687.

Khatiwala, S., F. Primeau, and T. Hall (2009), Reconstruction of the history of anthropogenic CO_2 concentrations in the ocean, *Nature*, *462*(7271), 346–349, doi:10.1038/nature08526.

Le Quéré, C., et al. (2007), Saturation of the Southern Ocean CO_2 sink due to recent climate change, *Science*, *316*(5832), 1735–1738, doi:10.1126/science.1136188.

Long, M. C., K. Lindsay, S. Peacock, J. K. Moore, and S. C. Doney (2013), Twentieth-century oceanic carbon uptake and storage in CESM1(BGC)*, *J. Clim.*, *26*(18), 6775–6800, doi:10.1175/JCLI-D-12-00184.1.

Lovenduski, N. S., M. C. Long, P. R. Gent, and K. Lindsay (2013), Multi-decadal trends in the advection and mixing of natural carbon in the Southern Ocean, *Geophys. Res. Lett.*, *40*, 139–142, doi:10.1029/2012GL054483.

Marshall, J., and K. Speer (2012), Closure of the meridional overturning circulation through Southern Ocean upwelling, *Nat. Geosci.*, *5*(3), 171–180, doi:10.1038/ngeo1391.

Meijers, A. J. S. (2014), The Southern Ocean in the Coupled Model Intercomparison Project Phase 5, *Philos. Trans. R. Soc., A*, *372*(2019), doi:10.1098/rsta.2013.0296.

Meredith, M. P., and A. M. Hogg (2006), Circumpolar response of Southern Ocean eddy activity to a change in the Southern Annular Mode, *Geophys. Res. Lett.*, *33*, L16608, doi:10.1029/2006GL026499.

Meredith, M. P., A. C. N. Garabato, A. M. Hogg, and R. Farneti (2012), Sensitivity of the overturning circulation in the Southern Ocean to decadal changes in wind forcing, *J. Clim.*, *25*(1), 99–110, doi:10.1175/2011jcli4204.1.

Mignone, B. K., A. Gnanadesikan, J. L. Sarmiento, and R. D. Slater (2006), Central role of Southern Hemisphere winds and eddies in modulating the oceanic uptake of anthropogenic carbon, *Geophys. Res. Lett.*, *33*, L01604, doi:10.1029/2005GL024464.

Moore, J. K., K. Lindsay, S. C. Doney, M. C. Long, and K. Misumi (2013), Marine Ecosystem Dynamics and Biogeochemical Cycling in the Community Earth System Model [CESM1(BGC)]: Comparison of the 1990s with the 2090s under the RCP4.5 and RCP8.5 scenarios, *J. Clim.*, *26*(23), 9291–9312, doi:10.1175/JCLI-D-12-00566.1.

Sabine, C. L., et al. (2004), The oceanic sink for anthropogenic CO_2, *Science*, *305*(5682), 367–371, doi:10.1126/science.1097403.

Sallee, J. B., R. J. Matear, S. R. Rintoul, and A. Lenton (2012), Localized subduction of anthropogenic carbon dioxide in the Southern Hemisphere oceans, *Nat. Geosci.*, *5*(8), 579–584, doi:10.1038/ngeo1523.

Sarmiento, J. L., T. M. C. Hughes, R. J. Stouffer, and S. Manabe (1998), Simulated response of the ocean carbon cycle to anthropogenic climate warming, *Nature*, *393*(6682), 245–249, doi:10.1038/30455.

Thompson, D. W. J., S. Solomon, P. J. Kushner, M. H. England, K. M. Grise, and D. J. Karoly (2011), Signatures of the Antarctic ozone hole in Southern Hemisphere surface climate change, *Nat. Geosci.*, *4*(11), 741–749, doi:10.1038/ngeo1296.

Waugh, D. W., F. Primeau, T. DeVries, and M. Holzer (2013), Recent changes in the ventilation of the Southern Oceans, *Science*, *339*(6119), 568–570, doi:10.1126/science.1225411.